

Damping modification factor of pseudo-acceleration spectrum considering influences of magnitude, distance and site conditions

Haizhong Zhang^{1a}, Jia Deng² and Yan-Gang Zhao^{*3}

¹Eco-Science Course, Faculty of Agriculture, Yamagata University, 1-23, Wakaba-machi, Tsuruoka-shi, Yamagata 997-8555, Japan

²China Academy of Building Research Co., Ltd, Beijing, 100013, China

³Key Laboratory of Urban Security and Disaster Engineering of Ministry of Education, Beijing University of Technology, Beijing, 100124, China

(Received May 27, 2023, Revised September 25, 2023, Accepted September 28, 2023)

Abstract. The damping modification factor (DMF) is used to modify the 5%-damped response spectrum to produce spectral values that correspond to other necessary damping ratios for seismic design. The DMF has been the subject of numerous studies, and it has been discovered that seismological parameters like magnitude and distance can have an impact on it. However, DMF formulations incorporating these seismological parameters cannot be directly applied to seismic design because these parameters are not specified in the present seismic codes. The goal of this study is to develop a formulation for the DMF that can be directly applied in seismic design and that takes the effects of magnitude, distance, and site conditions into account. To achieve this goal, 16660 ground motions with magnitudes ranging from 4 to 9 and epicentral distances ranging from 10 to 200 km are used to systematically study the effects of magnitude, distance, and site conditions on the DMF. Furthermore, according to the knowledge that magnitude and distance affect the DMF primarily by changing the spectral shape, a spectral shape factor is adopted to reflect influences of magnitude and distance, and a new formulation for the DMF incorporating the spectral shape factor is developed. In comparison to the current formulations, the proposed formulation provides a more accurate prediction of the DMF and can be employed directly in seismic design.

Keywords: damping modification factor; distance; magnitude; response spectrum; site conditions; spectral shape factor

1. Introduction

The majority of seismic design codes, such as Eurocode 8 (2004) and ASCE 7-10 (2011), typically characterize earthquake action as a pseudo-acceleration response spectrum with a damping ratio of 5% (Zhao and Zhang 2017, Zhang and Zhao 2021b). Similarly, ground motion prediction equations for the pseudo-acceleration response spectrum are also typically developed at a damping ratio of 5% (Douglas 2003). In reality, however, structural systems can have damping ratios greater than 5%, such as structures with energy dissipation devices or isolation systems. For such cases, the damping modification factor (DMF) is necessary to modify the 5%-damped response spectrum to obtain spectral values for other damping ratios for seismic design. Researchers have worked extensively on DMF over the past few decades and have put out a wide variety of formulations. Newmark and Hall (1982) conducted the first study of DMF based on a small number of earthquake records in the United States before 1973. They developed a DMF formulation applicable for damping ratios less than 20%. This formulation consists of three parts: the acceleration-, velocity-, and displacement-sensitive regions.

This formulation has been used in many later seismic design standards, such as ATC-40 (1996) and FEMA-273 (1997). Using 206 strong ground motion records from Japan, Kawashima and Aizawa (1986) developed a DMF formulation that is applicable for damping ratios between 5% and 10%. Ashour (1987) developed a DMF formulation by analyzing 6 structural periods and 11 damping ratios using real and synthetic earthquake motions. In each of the DMF formulations mentioned above, a single parameter, i.e., the damping ratio, is included. Similarly, several DMF formulations that only include the damping ratio have been developed using various earthquake databases (Bommer *et al.* 2000, Tolis and Faccioli 1999).

Numerous investigations have discovered that the DMF is also influenced by the natural period of the structure in addition to the damping ratio, including Wu and Hanson (1989), Lin and Chang (2003), Atkinson and Pierre (2004), and Cardone *et al.* (2009). Surana *et al.* (2019) constructed a DMF formulation taking into account the structure's natural period and damping ratio based on 203 horizontal acceleration records collected between 1986 and 2001 from the Indian strong-motion database. Lin *et al.* (2005) proposed a DMF formulation that takes the structural period and damping ratio into account based on 216 ground motions recorded at firm sites in California. Likewise, many DMF formulations that take structural period and damping ratio into account have been developed using various earthquake databases (Baizid and Malek 2018, Benahmed 2018, Castillo and Ruiz 2014, Daneshvar and Bouaanani

*Corresponding author, Professor

E-mail: zhaoyg@bjut.edu.cn

^aAssociate Professor

E-mail: zhang@tds1.tr.yamagata-u.ac.jp

2017, Fernandez-Davila and Mendo 2020, Mollaioli *et al.* 2014, Sadek *et al.* 2000).

Numerous research conducted recently discovered that DMF also depends on a variety of other factors, including site conditions, magnitude, distance, ground-motion duration, type, etc., in addition to structural period and damping ratio. Lin and Chang (2004) constructed a DMF formulation considering site conditions based on site classification using 1037 acceleration records of ground motions in the Pacific Earthquake Engineering Research Center (PEER). Similarly, Lin (2007) constructed a DMF formulation that takes site conditions into account based on site classification using 338 acceleration records from the Chi-Chi earthquake in Taiwan. Zhou and Zhao (2020) developed a DMF formulation considering site conditions using 4695 ground motion records from 136 subduction slab earthquakes in the Strong-motion Seismograph Networks (K-NET, KiK-net) of Japan (NIED 1995). In addition, Palermo *et al.* (2016) proposed a simple DMF formulation that incorporates the ratio between the structural period and the site-predominant period. Additionally, Li and Chen (2017) used the K-NET and KiK-net database's thousands of earthquake recordings to construct a DMF formulation that takes magnitude and epicentral distance into account. Bommer and Mendis (2005) and Cameron and Green (2007) pointed out that the ground-motion duration also affects DMF. This conclusion is confirmed by Stafford *et al.* (2008), who also developed a DMF formulation taking into account the ground-motion duration. Rezaeian *et al.* (2014) further validated the significant impact of ground-motion duration on DMF based on seismic records from the NGA-West 2 project database. Conde-Conde and Benavent-Climent (2019) also developed a formulation that takes the ground-motion duration and site conditions into account based on 880 far-field accelerograms recorded in Europe. Anbazhagan *et al.* (2016) used 410 horizontal motions to thoroughly investigate the effects of all the aforementioned parameters on the DMF, including magnitude, hypocenter distance, site condition, damping ratio, structural period, and ground-motion duration. Hatziigeorgiou (2010) also studied the effects of artificial earthquakes on DMF. Khoshnoudian *et al.* (2014) used a set of 91 pulse-like near-fault ground motions to study the impacts of inertial soil-structure interaction on DMF subjected to such ground motions. Pu *et al.* (2016) studied the effects of pulse-like ground motions and developed DMF formulations for displacement, velocity, and acceleration spectra. Sheikh *et al.* (2013) used a variety of simulated ground-motion records to investigate the effects of earthquake shaking level, source-to-site distance, soil plasticity index, and bedrock rigidity on the DMF. Greco *et al.* (2018a) developed a method for estimating DMF using the random vibration theory and investigated a number of parameters that may affect DMF. Zhang and Zhao (2020) calculated the DMF and systematically investigated the impacts of magnitude, epicentral distance, and site conditions on the DMF using a source-based Fourier amplitude spectrum (FAS) model based on random vibration theory. Similar to this, many DMF formulations that consider site conditions, magnitude,

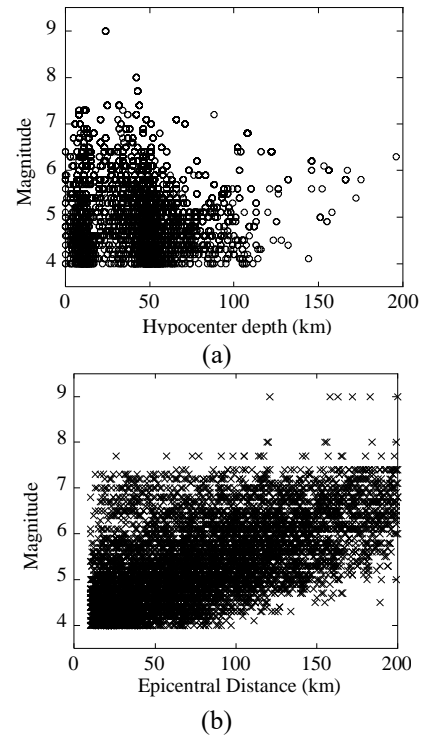


Fig. 1 Distributions of (a) Hypocenter depth and magnitude and (b) Epicentral distance and magnitude of selected seismic records

distance, and ground-motion duration and type have been developed using various earthquake records (Akkar 2014, Daneshvar *et al.* 2016, D'avalos *et al.* 2022, Greco *et al.* 2018b, Greco *et al.* 2019, Hao *et al.* 2011, Hubbard and Macroeidis 2011, Nagao 2015, Papagiannopoulos *et al.* 2013, Piscal 2018, Zhou *et al.* 2014, Zhao *et al.* 2019).

Although the aforementioned studies demonstrate that the DMF is influenced by seismological parameters like magnitude and distance, the existing codes do not provide these parameters, making it impossible to directly apply formulations including these parameters to seismic design. This study's goal is to develop a DMF formulation that can be directly used in seismic design and that takes the effects of site conditions, distance, and magnitude into account. The structure of this paper is organized as follows. In Section 2, 16660 ground motions recorded in 338 sites were chosen from the Strong-Motion Seismograph Networks K-NET and KiK-net. In Section 3, the effects of magnitude, epicentral distance, and site conditions on DMF were explored. In Section 4, regression analysis is performed to develop a DMF formulation that incorporates the effects of site conditions, distance, and magnitude. The formulation developed by this study is contrasted with formulations from earlier investigations in Section 5. Finally, the conclusions are outlined in Section 6.

2. Strong ground-motion records

To study the effects of magnitude, epicentral distance, and site conditions on DMF and construct a DMF

Table 1 Classification of the selected ground-motion records based on site conditions, magnitude, and epicentral distance

Site Class, $V_{s,30}$ (m/s)	Number	Magnitude, M	Number	Epicentral Distance, R (km)	Number		
B (760,1500]	1516	$4 \leq M < 5.5$	999	$10 \leq R < 50$	551		
				$50 \leq R < 100$	350		
				$100 \leq R \leq 200$	98		
		$5.5 \leq M < 6.5$	357	$10 \leq R < 50$	357	$10 \leq R < 50$	71
						$50 \leq R < 100$	149
						$100 \leq R \leq 200$	137
		$M \geq 6.5$	160	$10 \leq R < 50$	160	$10 \leq R < 50$	20
						$50 \leq R < 100$	51
						$100 \leq R \leq 200$	89
C (360,760]	2142	$4 \leq M < 5.5$	1288	$10 \leq R < 50$	663		
				$50 \leq R < 100$	489		
				$100 \leq R \leq 200$	136		
		$5.5 \leq M < 6.5$	509	$10 \leq R < 50$	509	$10 \leq R < 50$	82
						$50 \leq R < 100$	192
						$100 \leq R \leq 200$	235
		$M \geq 6.5$	345	$10 \leq R < 50$	345	$10 \leq R < 50$	51
						$50 \leq R < 100$	88
						$100 \leq R \leq 200$	206
D (180,360]	3209	$4 \leq M < 5.5$	1939	$10 \leq R < 50$	803		
				$50 \leq R < 100$	783		
				$100 \leq R \leq 200$	353		
		$5.5 \leq M < 6.5$	904	$10 \leq R < 50$	904	$10 \leq R < 50$	97
						$50 \leq R < 100$	284
						$100 \leq R \leq 200$	523
		$M \geq 6.5$	366	$10 \leq R < 50$	366	$10 \leq R < 50$	52
						$50 \leq R < 100$	58
						$100 \leq R \leq 200$	256
E (-,180]	1463	$4 \leq M < 5.5$	814	$10 \leq R < 50$	414		
				$50 \leq R < 100$	297		
				$100 \leq R \leq 200$	103		
		$5.5 \leq M < 6.5$	472	$10 \leq R < 50$	472	$10 \leq R < 50$	62
						$50 \leq R < 100$	139
						$100 \leq R \leq 200$	271
		$M \geq 6.5$	177	$10 \leq R < 50$	177	$10 \leq R < 50$	19
						$50 \leq R < 100$	34
						$100 \leq R \leq 200$	124

formulation, earthquake data were selected as much as possible to comprehensively cover cases considered in seismic design, while ensuring a balance in dataset size in terms of magnitudes, distances, and site conditions. A total of 16660 ground-motion accelerations from 8330 seismic records recorded in 338 sites in K-NET and KiK-net were chosen. The selected seismic records cover a wide range of magnitude, epicentral distance, and site conditions. The epicentral distance ranges from 10 km to 200 km, while the magnitude ranges from 4.0 to 9.0. The average shear-wave

velocity in the upper 30 m, $V_{s,30}$, of the stations varies from 106 to 1437 m/s, which covers the four site classes (B, C, D, and E) defined in the National Earthquake Hazards Reduction Program (NEHRP) (2000) and ASCE 7-10 (2011). Due to a lack of stations belonging to site class A in Japan, seismic motions recorded on such sites were not included. Additionally, the hypocenter depth of the chosen seismic data ranges from 0 km to 196 km, and the peak ground acceleration (PGA) ranges from 20.0 to 2599.9 gal. Fig. 1(a) shows the distribution of hypocenter depth and

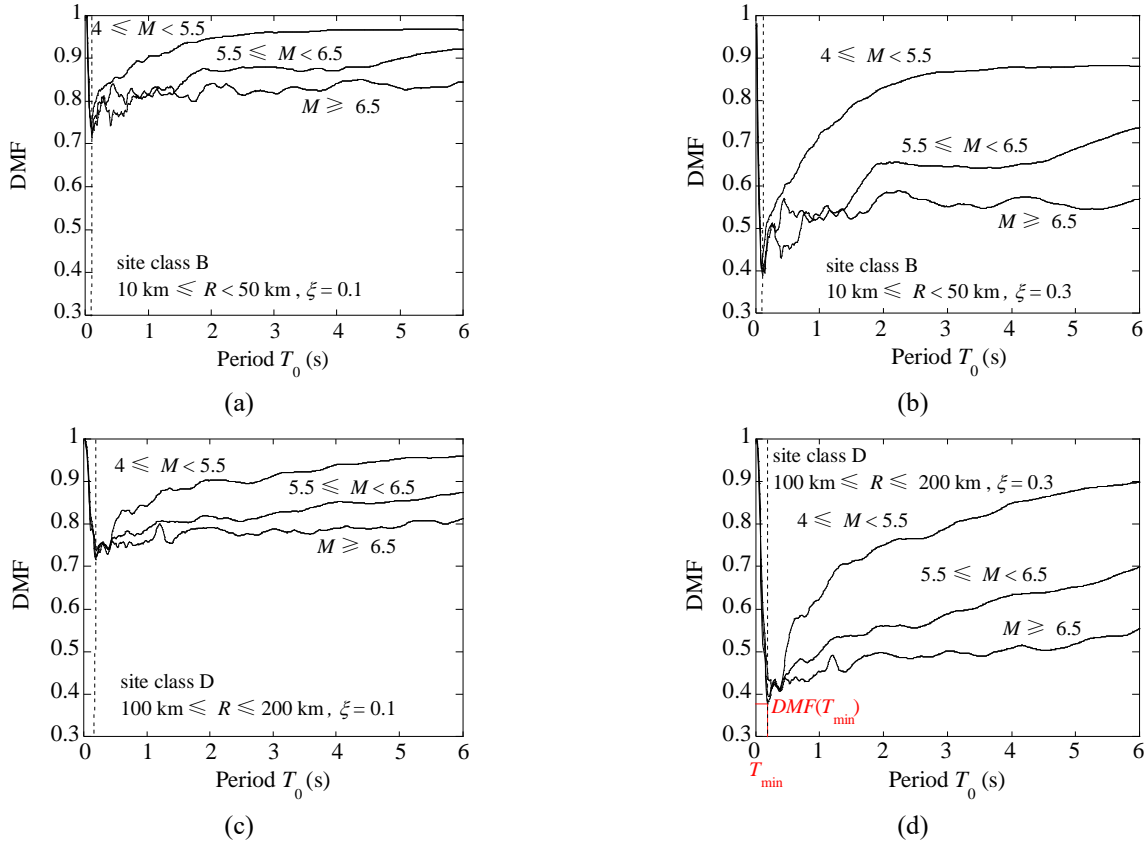


Fig. 2 The effect of magnitude on DMF for the cases (a) Site class B, $10 \text{ km} \leq R < 50 \text{ km}$, $\zeta = 0.1$, (b) Site class B, $10 \text{ km} \leq R < 50 \text{ km}$, $\zeta = 0.3$, (c) Site class D, $100 \text{ km} \leq R \leq 200 \text{ km}$, $\zeta = 0.1$ and (d) Site class D, $100 \text{ km} \leq R \leq 200 \text{ km}$, $\zeta = 0.3$

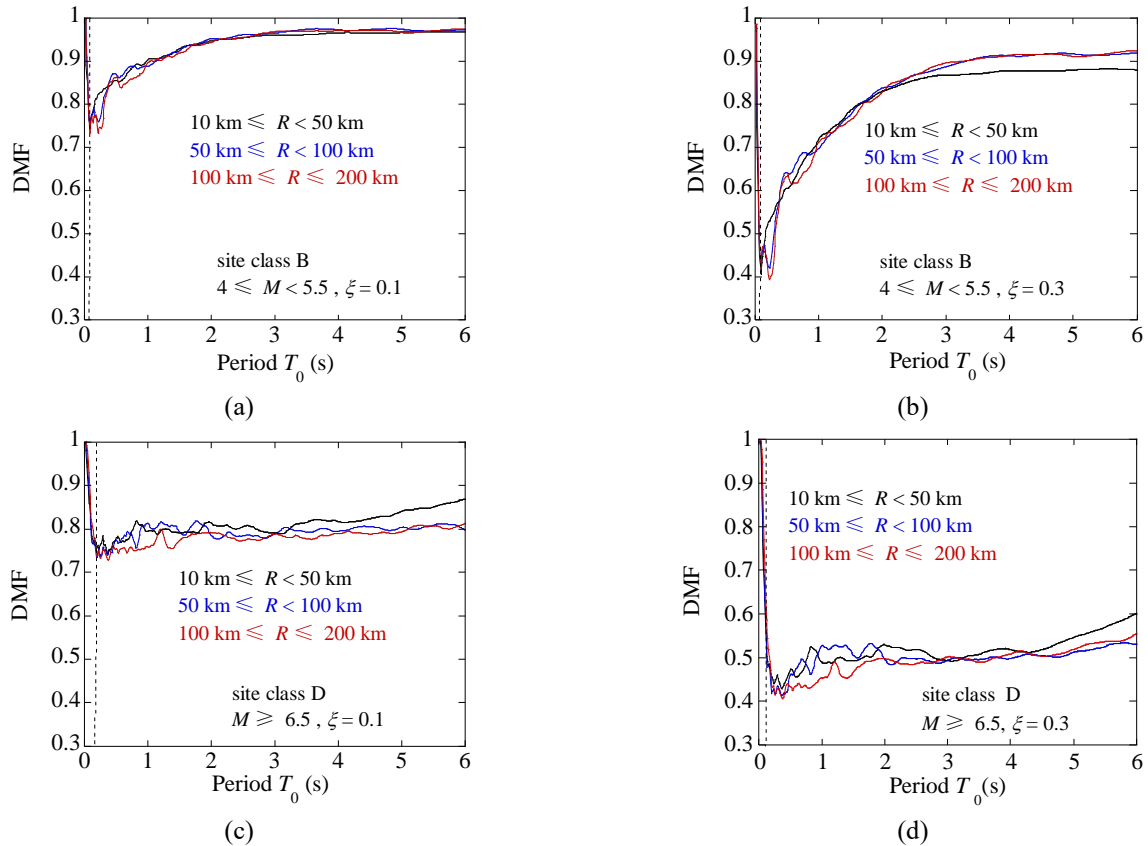


Fig. 3 The effect of epicentral distance on DMF for the cases (a) Site class B, $4.5 \leq M < 5.5$, $\zeta = 0.1$, (b) Site class B, $4.5 \leq M < 5.5$, $\zeta = 0.3$, (c) Site class D, $M \geq 6.5$ and $\zeta = 0.1$ and (d) Site class D, $M \geq 6.5$, $\zeta = 0.3$

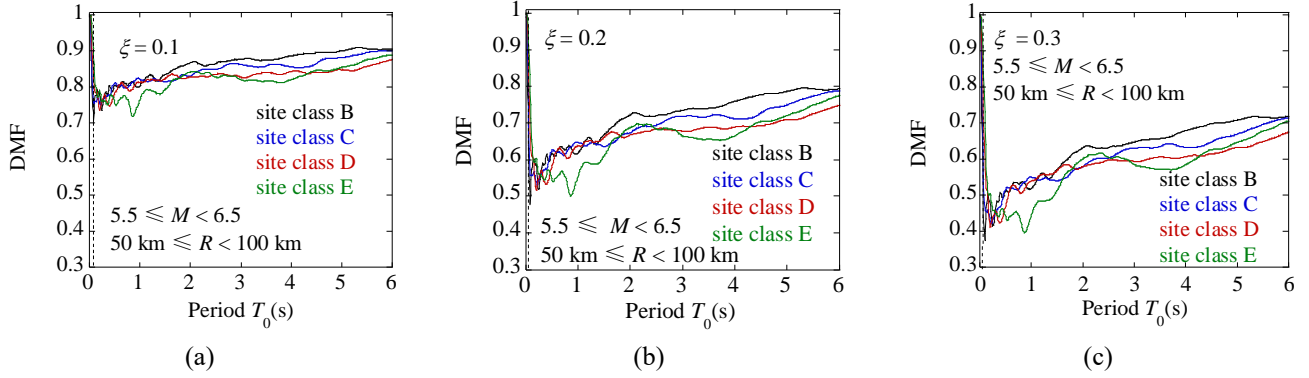


Fig. 4 The effects of site conditions on DMF for the cases (a) $\zeta=0.1$, (b) $\zeta=0.2$ and (c) $\zeta=0.3$

magnitude of selected seismic records, and Fig. 1(b) shows the distribution of epicentral distance and magnitude of selected seismic records.

In order to study the effect of site conditions on DMF, the selected seismic records are grouped according to the average shear-wave velocity at the top 30 m depth, $V_{S,30}$, which is defined as (NEHRP 2000)

$$V_{S,30}=30/[\sum (h_i/V_i)] \quad (1)$$

where, h_i is the thickness of the i th layer of soil, and V_i is the shear-wave velocity of the i th layer of soil. The KiK-net provides shear-wave velocities of soil deeper than 30 m, however, the K-NET only provides shear-wave velocities of soil up to 20 m. For the sites from K-NET, $V_{S,30}$ can be obtained by (Kanno *et al.* 2006)

$$V_{S,30}=1.13V_{S,20}+19.5 \quad (2)$$

In Eq. (2), $V_{S,20}$ is the average shear-wave velocity at the top 20 m depth, which can be obtained by

$$V_{S,20}=20/[\sum (h_i/V_i)] \quad (3)$$

According to the $V_{S,30}$, these 8330 seismic records were divided into four groups: B, C, D, and E. Each group was subsequently separated into nine subgroups based on the magnitude and epicentral distances to explore the impacts of magnitude and distance on DMF, as shown in Table 1.

3. Effects of magnitude, epicentral distance, and site conditions on DMF

The DMF values of selected ground-motion records in the previous section are calculated based on the following expression,

$$DMF=\frac{PSa(\zeta, T_0)}{PSa(5\%, T_0)}=\frac{Sd(\zeta, T_0)}{Sd(5\%, T_0)} \quad (4)$$

where, $PSa(5\%, T_0)$ and $PSa(\zeta, T_0)$ represent the pseudo-acceleration response spectra at damping ratios of 5% and ζ , respectively; $Sd(5\%, T_0)$ and $Sd(\zeta, T_0)$ represent the displacement response spectra at damping ratios of 5% and ζ , respectively. The displacement response spectra in Eq. (4) are calculated using the direct-integration method by Nigam and Jennings (1969). The computations take into account 600 structural periods ranging from 0.01

seconds to 6 seconds (interval is 0.01 seconds) and 4 damping ratios (0.05, 0.1, 0.2, and 0.3). Then, the DMF values in each group classified in Table 1 are averaged, and representative results are displayed in Figs. 2-4.

As demonstrated in Fig. 2, at long oscillator periods, DMF decreases with increasing magnitude, and the variation degree increases with increasing the damping ratio. However, DMF is essentially unaffected by magnitude for short oscillator periods. The dividing point being affected by magnitude or not corresponds to the minimum value of DMF, $DMF(T_{\min})$, where T_{\min} is the oscillator period corresponding to $DMF(T_{\min})$. In addition, Fig. 3 indicates that the epicentral distance slightly affects the DMF when $T_0 \geq T_{\min}$, and the effect increases with the increase of the damping ratio. The influence of epicentral distance on DMF, however, is not governed and is much less substantial than that of magnitude. Similar to the effect of the magnitude, when $T_0 < T_{\min}$, DMF remains almost unaffected by epicentral distance. It can be found from Fig. 4 that the site conditions slightly affect the DMF when $T_0 \geq T_{\min}$ and the effect increases with the increase of damping ratio. The effect of site conditions on DMF is not governed and is less substantial than that of magnitude. Similar to effects to the magnitude and epicentral distance, when $T_0 < T_{\min}$, DMF remains almost unaffected by site conditions.

The mechanism of the effects of magnitude, distance, and site conditions on the DMF has been systematically discussed by Zhang and Zhao (2020) based on random vibration theory. Zhang and Zhao (2020) pointed out that trends in the DMF with the variation of the oscillator period T_0 are mainly controlled by the shape of the FAS, and the overall shapes of the DMF and FAS are almost symmetrical with respect to the period axis. Since the ground-motion FAS varies with the magnitude, distance, and site conditions, the corresponding DMF also varies accordingly with these parameters.

Since the dependence of DMF on the magnitude, epicentral distance, and site conditions performs differently at $T_0 \geq T_{\min}$ and $T_0 < T_{\min}$, the DMF function forms should be different for the two intervals. Therefore, before the construction of a DMF formulation, it is necessary to clarify the properties of the division point (T_{\min} , $DMF(T_{\min})$). For this purpose, influences of magnitude, epicentral distance, and site conditions on T_{\min} are discussed. Fig. 5

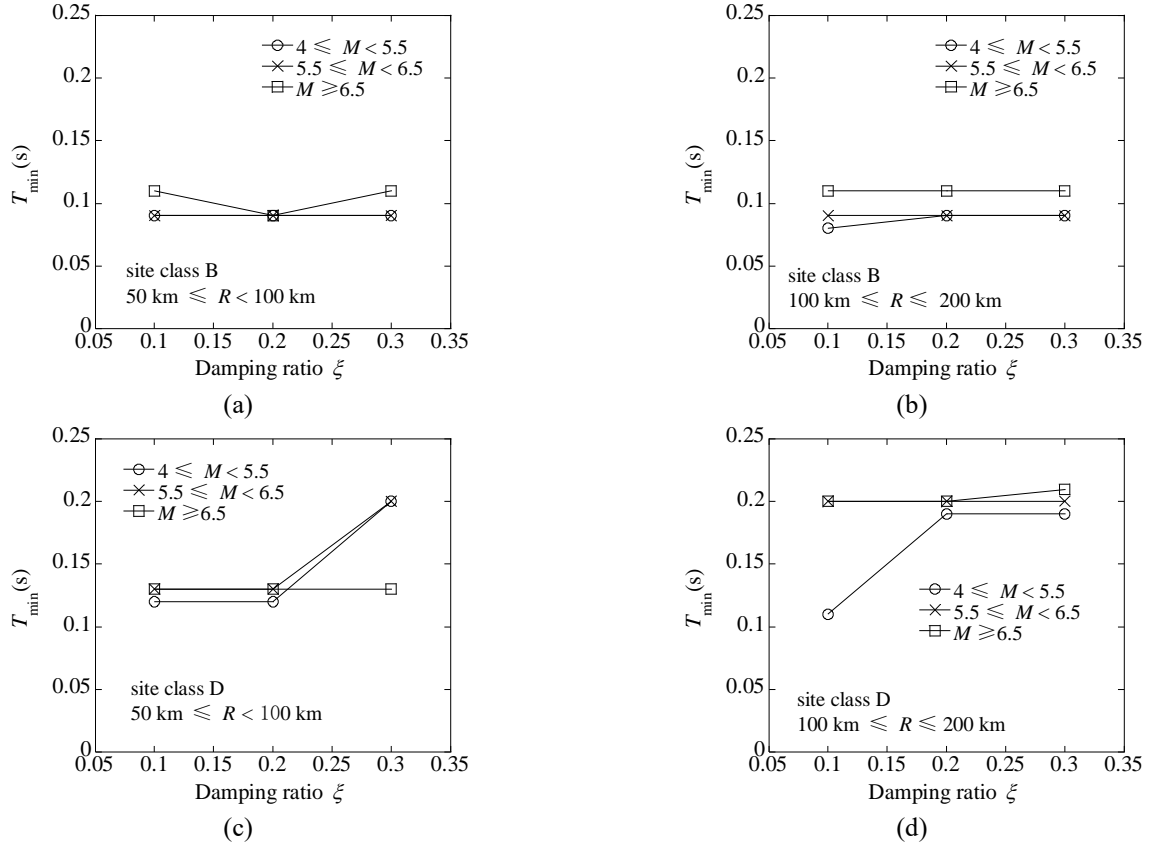


Fig. 5 The effect of magnitude on T_{min} for the cases (a) Site class B, $50 \text{ km} \leq R < 100 \text{ km}$, (b) Site class B, $100 \text{ km} \leq R \leq 200 \text{ km}$, (c) Site class D, $50 \text{ km} \leq R < 100 \text{ km}$ and (d) Site class D, $100 \text{ km} \leq R \leq 200 \text{ km}$

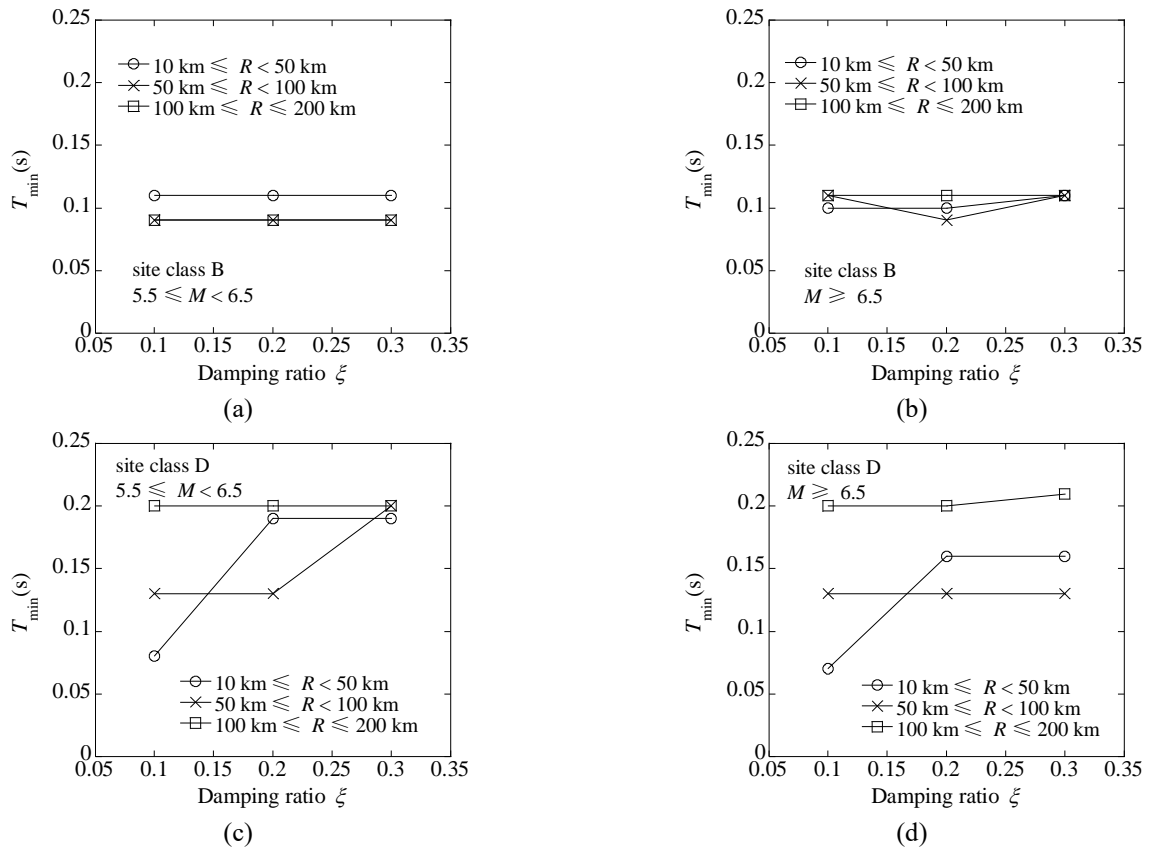


Fig. 6 The effect of epicentral distance on T_{min} for the cases (a) Site class B, $5.5 \leq M < 6.5$, (b) Site class B, $M \geq 6.5$, (c) Site class D, $5.5 \leq M < 6.5$ and (d) site class D, $M \geq 6.5$

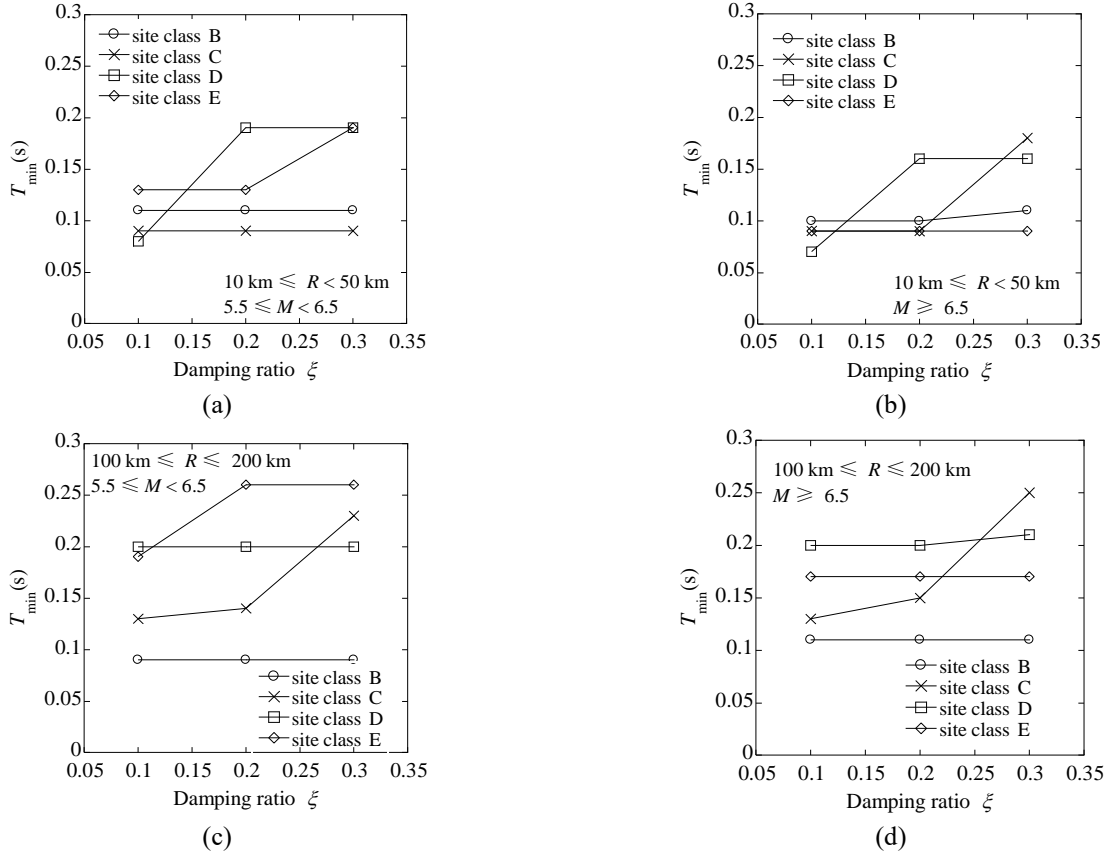


Fig. 7 The effects of site conditions on T_{\min} for the cases (a) $10 \text{ km} \leq R < 50 \text{ km}$, $5.5 \leq M < 6.5$, (b) $10 \text{ km} \leq R < 50 \text{ km}$, $M \geq 6.5$, (c) $100 \text{ km} \leq R \leq 200 \text{ km}$, $5.5 \leq M < 6.5$ and (d) $100 \text{ km} \leq R \leq 200 \text{ km}$, $M \geq 6.5$

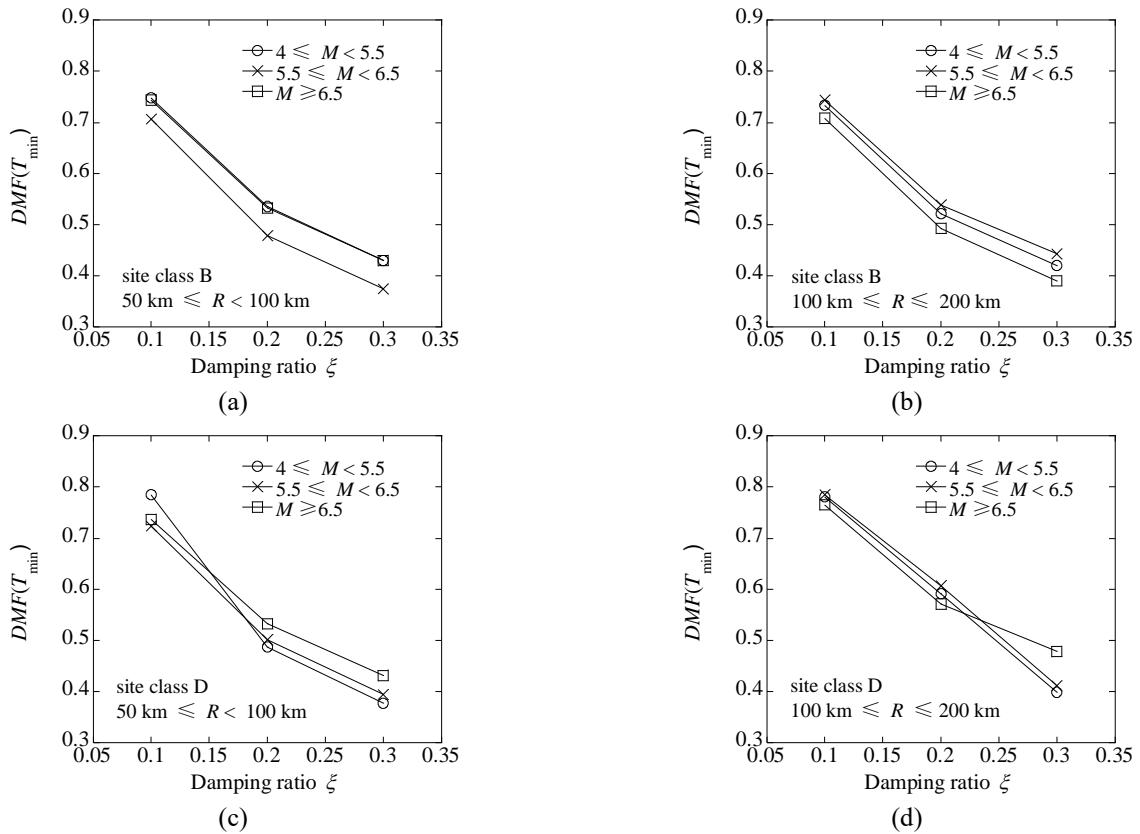


Fig. 8 The effects of magnitude on $DMF(T_{\min})$ for the cases (a) Site class B, $50 \text{ km} \leq R < 100 \text{ km}$, (b) Site class B, $100 \text{ km} \leq R \leq 200 \text{ km}$, (c) Site class D, $50 \text{ km} \leq R < 100 \text{ km}$ and (d) Site class D, $100 \text{ km} \leq R \leq 200 \text{ km}$

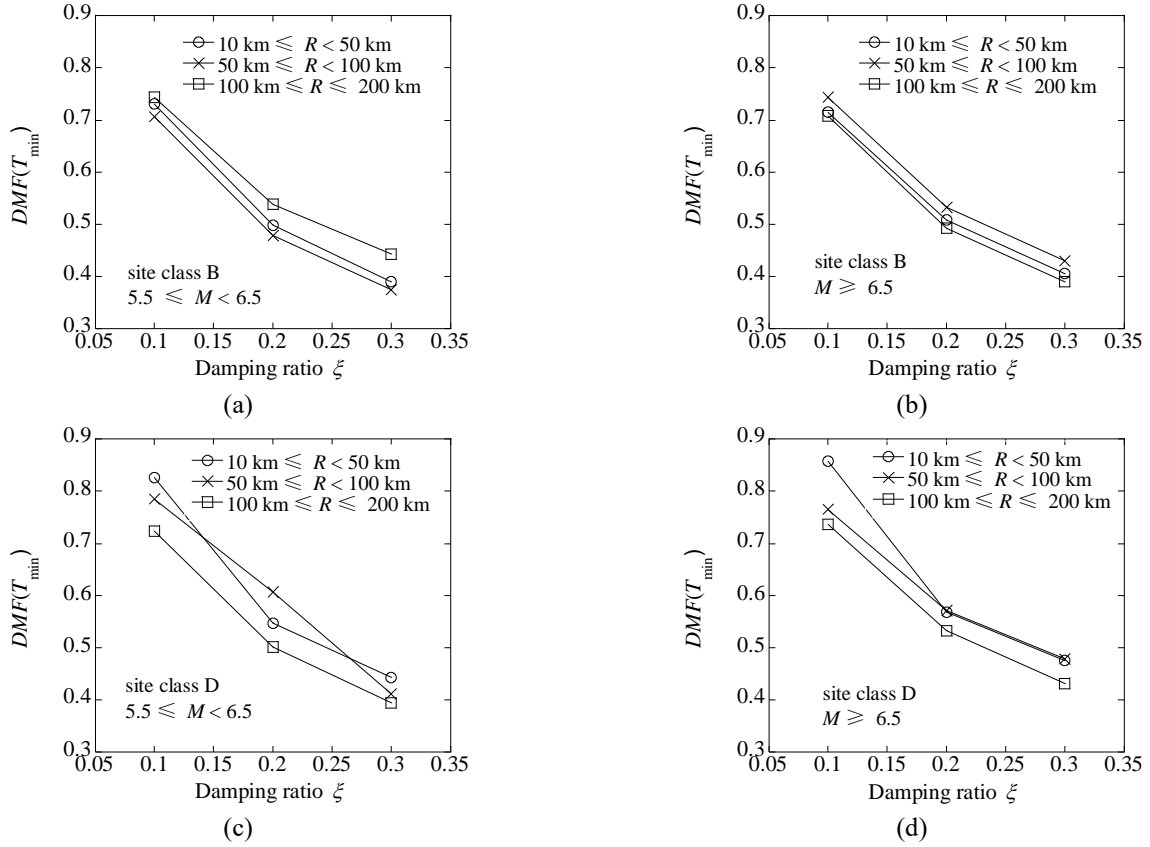


Fig. 9 The effects of epical distance on $DMF(T_{min})$ for the cases (a) Site class B, $5.5 \leq M < 6.5$, (b) Site class B, $M \geq 6.5$, (c) Site class D, $5.5 \leq M < 6.5$ and (d) Site class D, $M \geq 6.5$

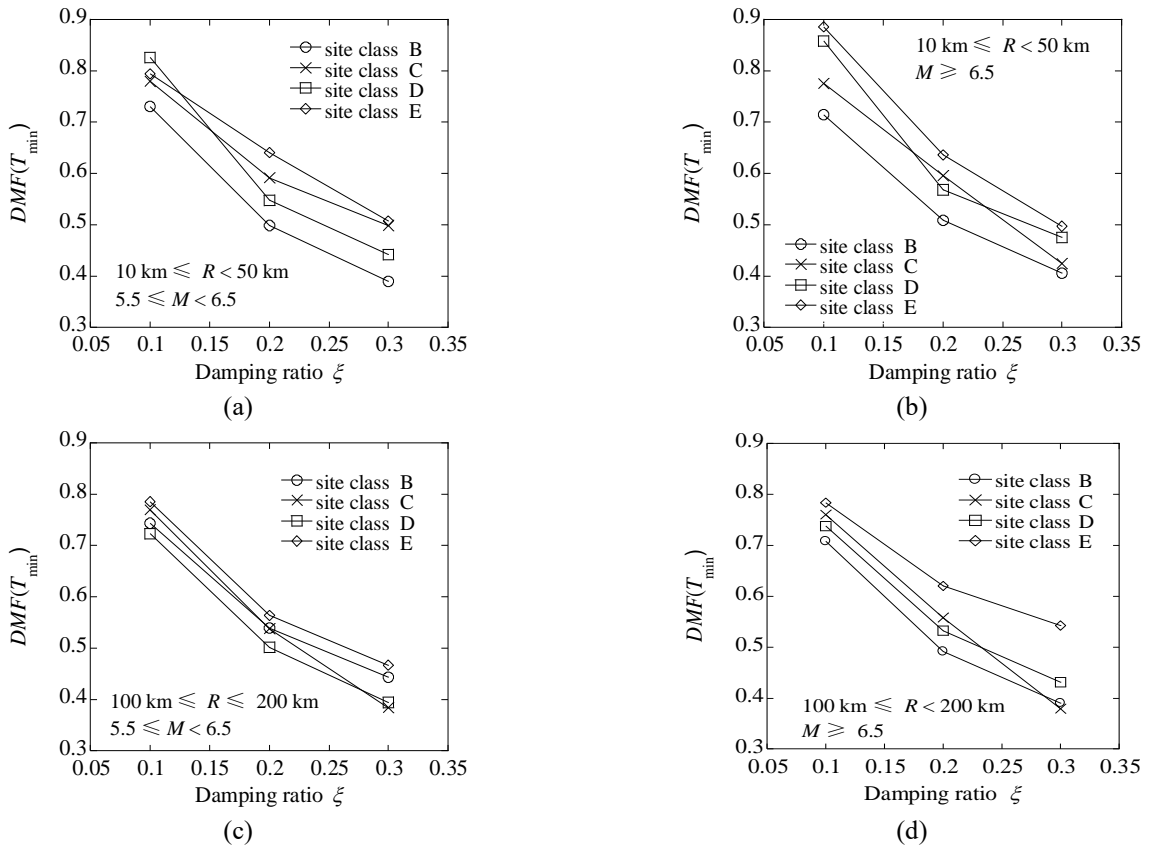


Fig. 10 The effects of site conditions on $DMF(T_{min})$ for the cases (a) $10 \text{ km} \leq R < 50 \text{ km}$, $5.5 \leq M < 6.5$, (b) $10 \text{ km} \leq R < 50 \text{ km}$, $M \geq 6.5$, (c) $100 \text{ km} \leq R \leq 200 \text{ km}$, $5.5 \leq M < 6.5$ and (d) $100 \text{ km} \leq R \leq 200 \text{ km}$, $M \geq 6.5$

demonstrates that although the relationship between T_{\min} and magnitude is not perfectly regular, in most cases, the higher the magnitude, the larger the T_{\min} value will be. Similarly, it can be seen from Fig. 6 that the fluctuation trend of T_{\min} with epicentral distance is also not always regular, but in the majority of situations, the T_{\min} value will be higher the farther away the epicenter is. Fig. 7 demonstrates that, in most cases, the bigger the T_{\min} , the softer the site is, albeit the relationship between the two is not always linear. These results indicate that the T_{\min} formulation can be simply considered as an increasing function of the magnitude, epicentral distance, and site classes.

Moreover, influences of magnitude, epicentral distance, and site conditions on $DMF(T_{\min})$ are also discussed. Fig. 8 demonstrates that the $DMF(T_{\min})$ variation with magnitude is relatively small and that the trend is erratic. Fig. 9 demonstrates that while in some cases (Figs. 9(c) and (d)), the variation of $DMF(T_{\min})$ with epicentral distance is more than that with magnitude, for the majority of cases, the variation degree is still not that high. Similar to this, even if some cases (Figs. 10(a) and (b)) show that the effect of site conditions on $DMF(T_{\min})$ is greater than that with magnitude, the maximum variation of $DMF(T_{\min})$ with site conditions does not surpass 0.2. These results indicate that the $DMF(T_{\min})$ formulation can be constructed independently of the magnitude, epicentral distance, and site classes, allowing for some margin of error.

4. Proposed DMF formulation

4.1 Parameters reflecting the spectral shape

Since different design response spectra incorporate contributions from earthquake data with different magnitudes, distances, and site conditions, while the DMF varies with these seismological parameters as discussed above, DMF values of different response spectra should indeed differ even for the same structural periods and damping ratios. To consider influences of magnitude, epicentral distance, and site conditions on DMF, in principle, all of these parameters should be included in the DMF formulation. However, the DMF formulation incorporating these parameters cannot be immediately applied to seismic design because the magnitude and epicentral distance are not stated as elements of seismic action in current seismic codes. To reflect the effects of magnitude and distance, it is important to identify a parameter that may be derived from the most recent seismic codes.

Zhang and Zhao (2020) reported that the primary way in which magnitude and epicentral distance have an impact on DMF is through altering the spectral shape. Craifaleanu (2013) investigated several variables for assessing the spectral shape, which are expressed as

$$T_c^* = \lambda_1^* / \lambda_0^* \quad (5)$$

$$T_{cen}^* = \sqrt{\lambda_2^* / \lambda_0^*} \quad (6)$$

$$\Omega = \sqrt{1 - \frac{(\lambda_2^*)^2}{\lambda_0^* \cdot \lambda_2^*}} \quad (7)$$

where, λ_0^* , λ_1^* , and λ_2^* can be obtained using the following equations,

$$\lambda_0^* = \sum_{i=1}^n S_{v,i}^2 \cdot \Delta T \quad (8)$$

$$\lambda_1^* = \sum_{i=1}^n T_i \cdot S_{v,i}^2 \cdot \Delta T \quad (9)$$

$$\lambda_2^* = \sum_{i=1}^n T_i^2 \cdot S_{v,i}^2 \cdot \Delta T \quad (10)$$

In Eqs. (8)-(10), S_v is the velocity response spectrum, ΔT is the period interval of the horizontal ordinate of S_v , which was adopted as 0.01 in this paper, T_i is the i th oscillator period, $S_{v,i}$ is the velocity spectral value corresponding to T_i , and n is the number of periods considered in the calculation of S_v .

Zhang and Zhao (2022a) also proposed another spectral shape parameter, p , which is expressed as

$$p = PSa(6s) / PGA \quad (11)$$

in which $PSa(6s)$ is the value of the pseudo-acceleration response spectrum at 6s.

4.2 The DMF formulation

As is known, the DMF value decreases with the increase of the structural period when $T_0 < T_{\min}$, and increases with the increase of the structural period when $T_0 \geq T_{\min}$. In addition, according to the analysis results of Section 3, when $T_0 < T_{\min}$, the DMF is controlled by the structural period and damping ratio, and nearly unaffected by magnitude, distance, and site conditions. However, when $T_0 \geq T_{\min}$, the DMF is not only affected by the structural period and damping ratio, but also affected by magnitude, distance, and site conditions. Therefore, the DMF formulation uses a piecewise function with $T_0 = T_{\min}$ as the division point. By testing numerous functional forms and striking a balance between simplicity and correctness, a formulation for the DMF that incorporates impacts of magnitude, epicentral distance, and site condition is proposed as,

$$DMF() = \begin{cases} 1 + \frac{DMF(T_{\min}) - 1}{T_{\min}} T_0 & T_0 < T_{\min} \\ 1 - \frac{1 - DMF(T_{\min})}{k_0(T_0 - T_{\min})^c + 1} & T_0 \geq T_{\min} \end{cases} \quad (12)$$

where, k_0 and c are parameters controlling the increasing rate of DMF with the period at $T_0 \geq T_{\min}$, they are used to reflect effects of magnitude, epicentral distance, and site condition. Since when $T_0 < T_{\min}$, the DMF is almost unaffected by magnitude, distance, and site conditions, Eq. (12) is independent of these parameters for $T_0 < T_{\min}$.

In Eq. (12), $DMF(T_{\min})$ is the minimum value of DMF, and T_{\min} is the period corresponding to $DMF(T_{\min})$. According to the results of Section 3, variations of $DMF(T_{\min})$ with magnitude, distance, and site conditions are small for most cases, and the variation trends are irregular. To simplify, $DMF(T_{\min})$ is considered a function of the

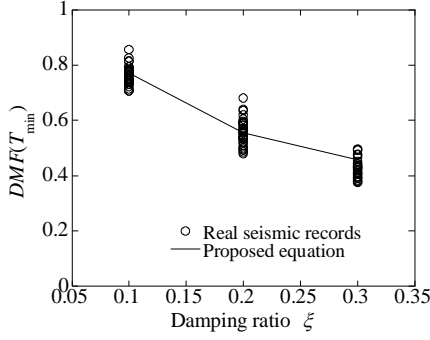
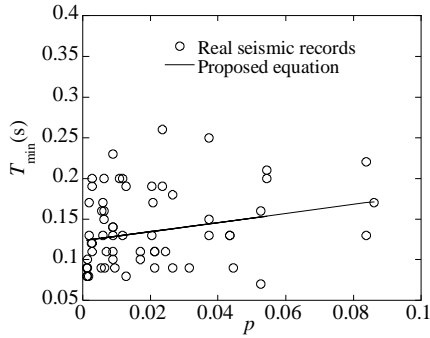

 Fig. 11 Variation of the $DMF(T_{\min})$ with the damping ratio

 Fig. 12 Variation of the period T_{\min} with spectral shape factor p

 Table 2 Values of a and b corresponding to different site classes

	B	C	D	E	Total
a	0.0008	0.0017	0.0012	0.0017	0.0055
b	0.8569	0.7009	0.8074	0.9107	0.567

damping ratio, which is regressed based on the least square method,

$$DMF(T_{\min})=0.22/(\xi^{0.53}) \quad (13)$$

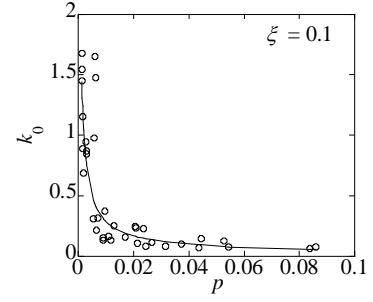
According to Fig. 11, Eq. (13) appears to perform well on the general trend. Additionally, the maximum relative error is limited to 22%, and relative errors for 79% of the results are less than 10%.

Since T_{\min} is slightly affected by magnitude and distance for most cases, T_{\min} is considered as a function of spectral shape factor reflecting effects of these parameters, and it is also regressed based on the least square method,

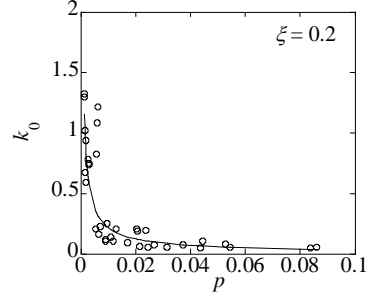
$$T_{\min}=4.52p+0.27 \quad (14)$$

In Eq. (14), the spectral shape factor p is used. In reality, the four spectral shape factors, T_c^* , T_{cen}^* , Ω , and p were all tested in the construction of DMF formulation, and the spectral shape factor p performs best, which will be detailed below. Although Fig. 12 shows a large scatter in T_{\min} , its effect on the final results of DMF is limited as can be seen in Section 4.3.

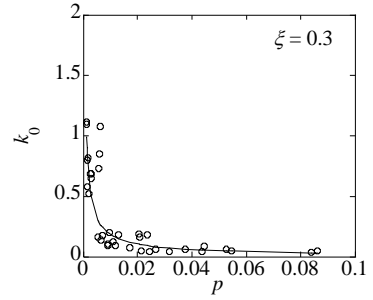
In Eq. (12), the parameters k_0 and c control the increasing rate of DMF with the structural period for $T_0 \geq T_{\min}$. Their values are determined by best-fitting the



(a)



(b)



(c)

 Fig. 13 Comparison of k_0 values obtained by Eq. (15) with observed results

DMF results in each group shown in Table 1, using the function form of Eq. (12) at $T_0 \geq T_{\min}$ based on the least square method. Since the parameters k_0 and c are affected by magnitude, distance, and site conditions, k_0 and c are considered as functions of the spectral shape factor p . In addition, it is found that the damping ratio also affects k_0 and c , therefore, k_0 is regressed as

$$k_0 = \frac{a}{p^{b \times \xi}} \quad (15)$$

where, a and b are regression coefficients, their values corresponding to different site conditions are shown in Table 2. Fig. 13 compares the k_0 values produced by Eq. (15) with observed results. It is observed that Eq. (15) performs exceptionally well in k_0 prediction. In addition, the values of c corresponding to different spectral shape factor p values, site conditions, and damping ratios are shown in Table 3.

4.3 Comparison with results of real seismic records

The DMF values are calculated using Eq. (12) and contrasted with those from actual seismic recordings to

Table 3 Values of c corresponding to different spectral shape factor p values, site classes and damping ratios

Site classes	$\ln p$	c		
		$\zeta=0.1$	$\zeta=0.2$	$\zeta=0.3$
B	-6.57	0.72	0.90	0.95
	-6.68	0.88	1.03	1.18
	-6.70	0.84	1.10	1.20
	-4.95	0.80	1.00	1.05
	-5.21	0.52	0.75	0.86
	-5.03	0.36	0.71	0.84
	-4.07	0.50	0.72	0.78
	-3.85	0.46	0.72	0.78
	-3.71	0.55	0.80	0.88
C	-6.27	0.84	1.12	1.24
	-6.50	0.76	1.02	1.16
	-6.39	0.96	1.28	1.42
	-4.66	0.92	1.32	1.42
	-4.72	0.70	0.98	1.08
	-4.71	0.28	0.76	0.88
	-3.63	0.46	0.78	0.98
	-3.46	0.40	0.72	0.80
	-3.29	0.48	0.88	0.96
D	-5.94	0.82	1.24	1.38
	-5.86	0.74	0.98	1.15
	-5.88	0.78	1.12	1.32
	-4.35	0.80	1.12	1.32
	-4.44	0.38	0.84	0.96
	-4.51	0.34	0.84	1.04
	-2.94	1.12	1.32	1.38
	-3.13	0.48	0.80	0.94
	-2.91	0.56	0.98	1.16
E	-5.12	0.76	1.02	1.14
	-5.17	0.84	1.12	1.25
	-5.06	1.07	1.46	1.67
	-3.89	0.76	1.12	1.20
	-3.88	0.46	0.80	0.92
	-3.75	0.52	0.92	1.08
	-3.11	0.52	0.88	1.02
	-2.48	0.48	0.80	0.88
	-2.45	0.60	0.94	1.08

ascertain the proposed formulation's correctness. Some representative comparisons are shown in Fig. 14. For the majority of situations taken into consideration in this study, Eq. (12) provides a good overall estimation of DMF. The relative errors by the proposed DMF formulation at each structural period are calculated and the results from 0s to 6s are averaged. In addition, the other three spectral shape factors, T_c^* , T_{cen}^* and Ω were also tested in the construction of the DMF formulation, the representative average relative errors for cases of $\zeta=0.1$ were listed in Table 4. It is found

that the relative error using spectral shape factor p is minimal compared with those using the other three spectral shape factors for most cases, relative errors of 94% results are smaller than 5%, and the maximum average relative error is limited to 7%.

5. Comparison with previous formulations

The DMF results computed by Eq. (12) are contrasted

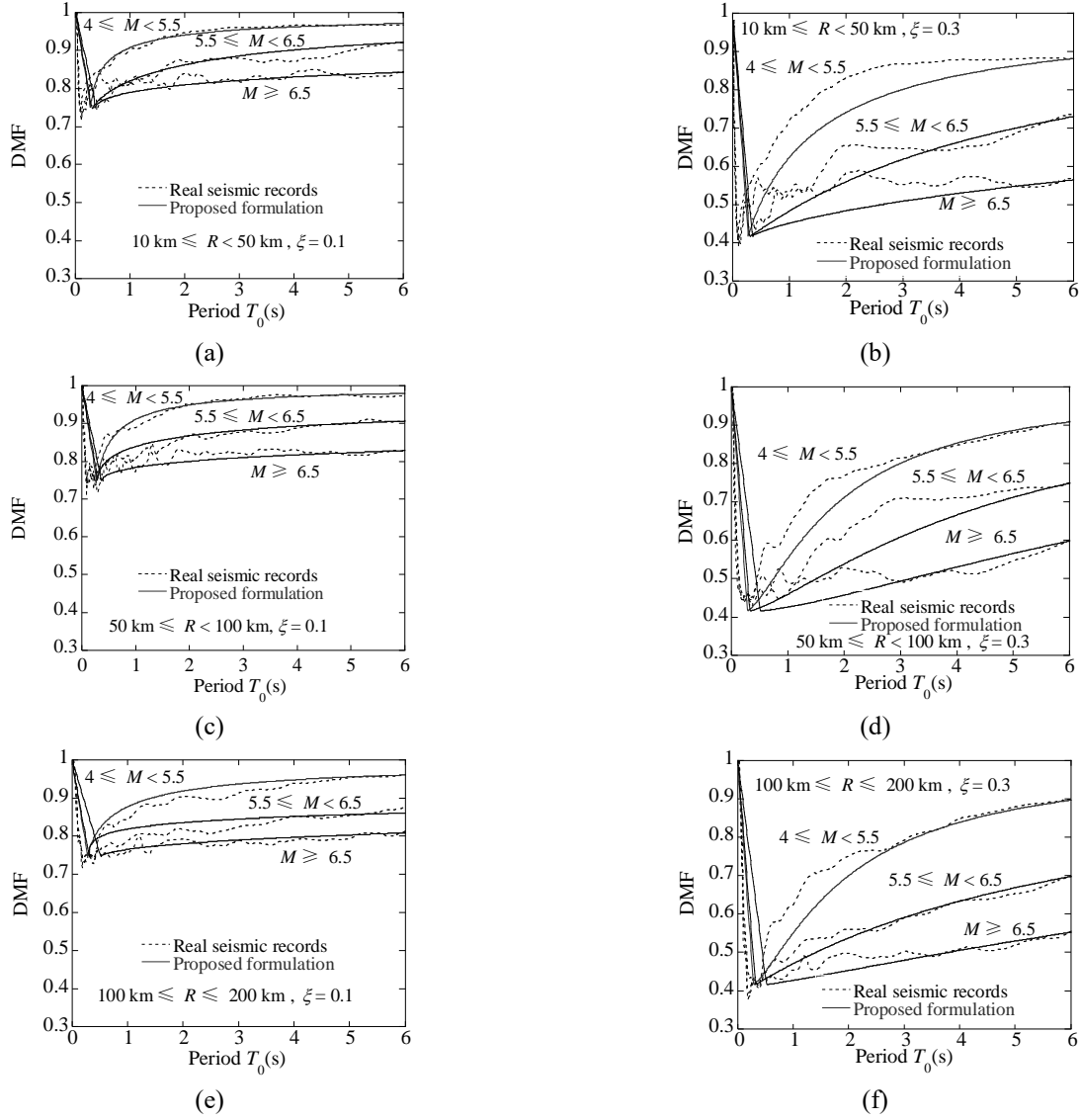


Fig. 14 Comparison of DMF values calculated by Eq. (12) and those of real seismic records for the cases (a) Site class B, $10 \text{ km} \leq R < 50 \text{ km}$, $\zeta = 0.1$, (b) Site class B, $10 \text{ km} \leq R < 50 \text{ km}$, $\zeta = 0.3$, (c) Site class B, $50 \text{ km} \leq R < 100 \text{ km}$, $\zeta = 0.1$, (d) Site class D, $10 \text{ km} \leq R < 50 \text{ km}$, $\zeta = 0.1$, (e) Site class D, $100 \text{ km} \leq R \leq 200 \text{ km}$, $\zeta = 0.1$ and (f) Site class D, $100 \text{ km} \leq R \leq 200 \text{ km}$, $\zeta = 0.3$

with the DMF results achieved by the DMF formulations of Benahmed (2018), Conde-Conde and Benavent-Climent (2019) as well as ASCE 7-22 (2022). The DMF formulation of Behnamed (2018) was constructed through nonlinear regression analyses of four sets of seismic records from PEER, which is a function of structural period and damping ratio.

$$DMF = 0.582 + 0.418 \times (12.279 - T)^{-3.9 \times (\zeta - 0.05)} \quad (16)$$

This formulation is suitable for cases with damping ratios less than 0.2, so damping ratios of 0.1 and 0.2 are considered for the comparison in this Section. The DMF formulation of Conde-Conde and Benavent-Climent (2019) was constructed using 880 seismic records from Europe, which is expressed as

$$DMF = \left[1 + \left(\sqrt{\frac{0.05 + \zeta}{0.10}} - 1 \right) \left(\frac{T_R}{T} \right)^\alpha \frac{T - T_R}{T} \right]^{-1} \quad (17)$$

where, T_R and α are coefficients that are obtained by nonlinear regression as listed in Table 2 of Conde-Conde and Benavent-Climent (2019). Their values corresponding to ground-motion duration longer than 16s were adopted, because ground-motion durations for most cases used for the comparison are longer than 16s. This formulation is applicable for $T_0 \leq 4 \text{ s}$, so only the cases of $T_0 \leq 4 \text{ s}$ are used for comparison.

As can be seen from Fig. 15, the proposed formulation can give a better estimation of DMF than the formulations of Benahmed (2018), Conde-Conde and Benavent-Climent (2019) as well as ASCE 7-22 (2022). In particular, the accuracies of DMF results obtained using Eq. (12) are much better than those of using the other three formulations for the cases with small magnitude (Figs. 15(a), (d), (g), and (j)). The results of the proposed formulation are very similar to those by formulations of Benahmed (2018), Conde-Conde and Benavent-Climent (2019), and ASCE 7-22

Table 4 Relative errors of DMF results calculated by Eq. (12) using different spectral shape factors ($\zeta=0.1$)

Site Class, $V_{s,30}$ (m/s)	Magnitude, M	Epicentral Distance, R (km)	p (%)	T_c^* (%)	T_{cen}^* (%)	Ω (%)	
B (760,1500]	$4 \leq M < 5.5$	$10 \leq R < 50$	0.07	2.12	1.15	2.76	
		$50 \leq R < 100$	0.37	2.31	1.73	1.53	
		$100 \leq R \leq 200$	0.84	1.77	1.74	0.66	
	$5.5 \leq M < 6.5$	$10 \leq R < 50$	1.02	6.25	5.46	6.28	
		$50 \leq R < 100$	1.21	6.51	4.51	5.90	
		$100 \leq R \leq 200$	0.06	7.26	2.54	7.63	
	$M \geq 6.5$	$10 \leq R < 50$	0.16	11.84	10.75	10.02	
		$50 \leq R < 100$	0.43	12.82	13.60	10.58	
		$100 \leq R \leq 200$	0.35	13.83	15.05	11.88	
	C (360,760]	$4 \leq M < 5.5$	$10 \leq R < 50$	0.86	2.54	0.45	1.38
			$50 \leq R < 100$	0.65	2.49	0.49	1.24
			$100 \leq R \leq 200$	0.75	2.35	1.88	0.38
$5.5 \leq M < 6.5$		$10 \leq R < 50$	0.11	3.47	2.40	2.50	
		$50 \leq R < 100$	1.28	4.35	3.46	5.07	
		$100 \leq R \leq 200$	1.53	6.99	3.29	9.96	
$M \geq 6.5$		$10 \leq R < 50$	1.13	11.35	10.15	6.02	
		$50 \leq R < 100$	0.11	10.50	12.73	4.00	
		$100 \leq R \leq 200$	0.82	12.30	12.38	5.84	
D (180,360]		$4 \leq M < 5.5$	$10 \leq R < 50$	0.99	3.56	1.78	2.52
			$50 \leq R < 100$	0.40	2.49	1.57	0.78
			$100 \leq R \leq 200$	1.98	0.71	1.37	1.79
	$5.5 \leq M < 6.5$	$10 \leq R < 50$	0.79	3.72	1.17	4.12	
		$50 \leq R < 100$	1.07	5.71	4.74	6.09	
		$100 \leq R \leq 200$	2.03	6.99	2.16	8.67	
	$M \geq 6.5$	$10 \leq R < 50$	0.60	7.41	9.78	0.06	
		$50 \leq R < 100$	0.26	9.52	13.20	3.55	
		$100 \leq R \leq 200$	1.34	12.75	12.63	7.79	
	E (-,180]	$4 \leq M < 5.5$	$10 \leq R < 50$	1.58	2.42	0.18	3.21
			$50 \leq R < 100$	4.03	0.09	1.41	0.78
			$100 \leq R \leq 200$	4.05	0.52	0.90	1.95
$5.5 \leq M < 6.5$		$10 \leq R < 50$	3.02	5.19	4.71	5.39	
		$50 \leq R < 100$	4.35	7.14	5.42	8.41	
		$100 \leq R \leq 200$	4.14	6.50	2.06	9.21	
$M \geq 6.5$		$10 \leq R < 50$	0.58	7.16	5.05	6.52	
		$50 \leq R < 100$	2.10	14.28	16.01	6.18	
		$100 \leq R \leq 200$	2.15	13.74	12.94	8.87	

(2022) for cases with large magnitudes (Figs. 15(c), (i), and (l)). Since formulations of Behnamed (2018) and Conde-Conde and Benavent-Climent (2019) ignore effects of magnitude and distance, their results don't change with magnitude and distance, and perform not that well for the cases with small and moderate magnitude. The DMF results by the formulation of Behnamed (2018) are very similar to those by the formulation of ASCE 7-22 (2022) for all cases. Nevertheless, since Eq. (12) is based entirely on seismic records from Japan, its accuracy needs to be further discussed by including seismic records from different

regions in future studies.

6. Conclusions

This study systematically examined the effects of magnitude, distance, and site conditions on the damping modification factor (DMF) and proposed a DMF formulation that not only takes these factors into account but can also be used directly in seismic design. The results of this study contribute to improving the rationality of the

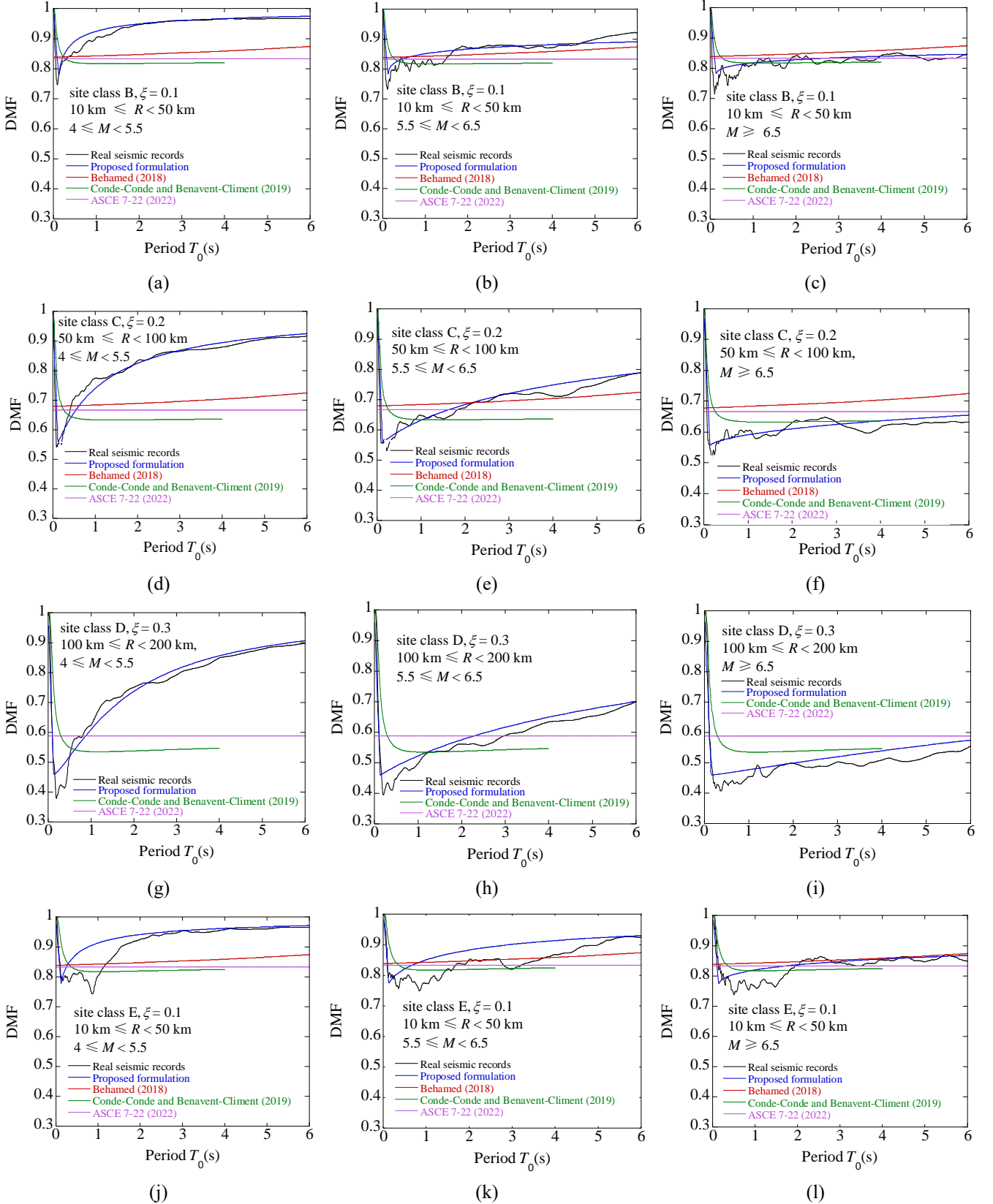


Fig. 15 Comparisons of the DMF results calculated by Eq. (12) with those obtained by formulations of Behamed (2018), Conde-Conde and Benavent-Climent (2019), and ASCE 7-22 (2022) for the cases (a) Site class B, $10 \text{ km} \leq R < 50 \text{ km}$, $4 \leq M < 5.5$, $\xi = 0.1$, (b) Site class B, $10 \text{ km} \leq R < 50 \text{ km}$, $5.5 \leq M < 6.5$, $\xi = 0.1$, (c) Site class B, $10 \text{ km} \leq R < 50 \text{ km}$, $M \geq 6.5$, $\xi = 0.1$, (d) Site class C, $50 \text{ km} \leq R < 100 \text{ km}$, $4 \leq M < 5.5$, $\xi = 0.2$, (e) Site class C, $50 \text{ km} \leq R < 100 \text{ km}$, $5.5 \leq M < 6.5$, $\xi = 0.2$, (f) Site class C, $50 \text{ km} \leq R < 100 \text{ km}$, $M \geq 6.5$, $\xi = 0.2$, (g) Site class D, $100 \text{ km} \leq R < 200 \text{ km}$, $4 \leq M < 5.5$, $\xi = 0.3$, (h) Site class D, $100 \text{ km} \leq R < 200 \text{ km}$, $5.5 \leq M < 6.5$, $\xi = 0.3$, (i) Site class D, $100 \text{ km} \leq R < 200 \text{ km}$, $M \geq 6.5$, $\xi = 0.3$, (j) Site class E, $10 \text{ km} \leq R < 50 \text{ km}$, $4 \leq M < 5.5$, $\xi = 0.1$, (k) Site class E, $10 \text{ km} \leq R < 50 \text{ km}$, $5.5 \leq M < 6.5$, $\xi = 0.1$ and (l) Site class E, $10 \text{ km} \leq R < 50 \text{ km}$, $M \geq 6.5$, $\xi = 0.1$

DMF formulation and enhancing its applicability in seismic design. The main conclusions of this study are summarized as follows.

- When $T_0 < T_{\min}$, the DMF is almost not affected by magnitude, epicentral distance, and site condition; when $T_0 \geq T_{\min}$, the DMF decreases with increasing magnitude, and the variation degree increases as the damping ratio is increased. When $T_0 \geq T_{\min}$, the epicentral distance and site conditions have a minor impact on the DMF, and the impact grows as the damping ratio increases. The effects of epicentral distance and site conditions on DMF, however, are not governed and are significantly less significant than those of magnitude.
- The spectral shape factor p performs the best among several other spectral shape factors to reflect effects of magnitude and distance. The DMF formulation incorporating the spectral shape factor can reasonably consider the effects of magnitude and distance.
- By comparing the proposed formulation's results with those from actual seismic data, it is discovered that it can provide a good prediction of DMF. And it is discovered that the new formulation can provide a superior estimation of DMF by comparison with earlier formulations.

Acknowledgments

This study was partially supported by the National Natural Science Foundation of China (Grant No. 52278135). This support is gratefully acknowledged. This study used strong-motion records from the Kyoshin net (K-NET) and Kiban–Kyoshin network (KiK-net). The authors are also grateful to Zheng Liu for assisting in the preparation of figure illustrations.

References

- Ashour, S.A. (1987), "Elastic seismic response of buildings with supplemental damping", Ph.D. Dissertation, Michigan University, Ann Arbor, MI, USA.
- ATC-40 (1996), Seismic Evaluation and Retrofit of Concrete Buildings, Applied Technology Council (ATC), Redwood City, CA, USA.
- Atkinson, G.M. and Pierre, J.R. (2004), "Ground motion response spectra in Eastern North America for different critical damping values", *Seismol. Res. Lett.*, **75**(4), 541-545. <https://doi.org/10.1785/gssrl.75.4.541>.
- ASCE 7-10 (2011), Minimum Design Loads for Buildings and Other Structures, American Society of Civil Engineers, Reston, VA, USA.
- ASCE 7-22 (2022), Minimum Design Loads for Buildings and Other Structures, American Society of Civil Engineers, Reston, VA, USA.
- Akkar, S., Sandikkaya, M.A. and Ay, B.Ö. (2014), "Compatible ground-motion prediction equations for damping scaling factors and vertical-to-horizontal spectral amplitude ratios for the broader Europe region", *Bull. Earthq. Eng.*, **12**, 517-547. <https://doi.org/10.1007/s10518-013-9537-1>.
- Anbazhagan, P., Uday, A., Moustafa, S.S.R. and Al-Arifi, N.S.N. (2016), "Pseudo-spectral damping reduction factors for the Himalayan Region considering recorded ground-motion data", *PLoS ONE*, **11**(9), e0161137. <https://doi.org/10.1371/journal.pone.0161137>.
- Bommer, J.J., Elnashai, A.S. and Weir, A.G. (2000), "Compatible acceleration and displacement spectra for seismic design codes", *Proceedings of the 12th World Conference on Earthquake Engineering*, Auckland, New Zealand, January-February.
- Bommer, J.J. and Mendis, R. (2005), "Scaling of spectral displacement ordinates with damping ratios", *Earthq. Eng. Struct. Dyn.*, **34** (2), 145-165. <https://doi.org/10.1002/eqe.414>.
- Baizid, B. and Malek, H. (2018), "Use of the artificial neural networks to estimate the DRF for Eurocode 8", *Period. Polytech. Civil Eng.*, **62**(2), 470-479. <https://doi.org/10.3311/PPci.8139>.
- Benahmed, B. (2018), "Formulation of damping reduction factor for the Algerian seismic code", *Asian J. Civil Eng.*, **19**, 375-385. <https://doi.org/10.1007/s42107-018-0023-6>.
- Conde-Conde, J. and Benavent-Climent, A. (2019), "Construction of elastic spectra for high damping", *Eng. Struct.*, **191**, 343-357. <https://doi.org/10.1016/j.engstruct.2019.04.047>.
- Cameron, W.I. and Green, R.A. (2007), "Damping correction factors for horizontal ground-motion response spectra", *Bull. Seism. Soc. Am.*, **97**(3), 934-960. <https://doi.org/10.1785/0120060034>.
- Cardone, D., Dolce, M. and Rivelli, M. (2009), "Evaluation of reduction factors for high-damping design response spectra", *Bull. Earthq. Eng.*, **7**, 273-291. <https://doi.org/10.1007/s10518-008-9097-y>.
- Castillo, T. and Ruiz, S.E. (2014), "Reduction factors for seismic design spectra for structures with viscous energy dampers", *J. Earthq. Eng.*, **18**(3), 323-349. <https://doi.org/10.1080/13632469.2013.860932>.
- Craifaleanu, I.G. (2013), "Investigation of the frequency content of ground motions recorded during strong Vrancea earthquakes, based on deterministic and stochastic indices", *Eighth International Conference on Structural Dynamics*, Leuven, Belgium, July.
- Douglas, J. (2003), "Earthquake ground motion estimation using strong-motion records: A review of equations for the estimation of peak ground acceleration and response spectral ordinates", *Earth. Sci. Rev.*, **61**, 43-104. [https://doi.org/10.1016/S0012-8252\(02\)00112-5](https://doi.org/10.1016/S0012-8252(02)00112-5).
- Daneshvar, P. and Bouaanani, N. (2017), "Damping modification factors for eastern Canada", *J. Seismol.*, **21**, 1487-1504. <https://doi.org/10.1007/s10950-017-9678-9>.
- Daneshvar, P., Bouaanani, N., Goda, K. and Atkinson, G.M. (2016), "Damping reduction factors for crustal, inslab, and interface earthquakes characterizing seismic hazard in southwestern British Columbia, Canada", *Earthq. Spectra*, **32**(1), 45-74. <https://doi.org/10.1193/061414EQS086M>.
- D'avalos, H., Miranda, E., Bantis, J. and Cruz, C. (2022), "Response spectral damping modification factors for structures built on soft soils", *Soil. Dyn. Earthq. Eng.*, **154**, 107153. <https://doi.org/10.1016/j.soildyn.2022.107153>.
- Eurocode 8 (2004), Design of Structures for Earthquake Resistance, Part 1: General Rules, Seismic Actions and Rules for Buildings, European Committee for Standardization, Brussels, Belgium.
- FEMA-273 (1997), NEHRP Guidelines for the Seismic Rehabilitation of Buildings, Federal Emergency Management Agency, Washington, D.C., USA.
- Fernandez-Davila, V.I. and Mendo, A.R. (2020), "Damping modification factors for the design of seismic isolation systems in Peru", *Earthq. Spectra*, **36**(4), 1-28. <https://doi.org/10.1177/875529302092618>.
- Greco, R., Fiore, A., Marano, G.C. and Briseghella, B. (2018a), "Effects of excitation bandwidth on damping reduction factor", *J. Earthq. Eng.*, **25**(4), 649-676.

- <https://doi.org/10.1080/13632469.2018.1528910>.
- Greco, R., Fiore, A. and Briseghella, B. (2018b), "Influence of soil type on damping reduction factor: A stochastic analysis based on peak theory", *Soil. Dyn. Earthq. Eng.*, **104**, 365-368. <https://doi.org/10.1016/j.soildyn.2017.10.020>.
- Greco, R., Vanzi, I., Lavorato, D. and Briseghella, B. (2019), "Seismic duration effect on damping reduction factor using random vibration theory", *Eng. Struct.*, **179**, 296-309. <https://doi.org/10.1016/j.engstruct.2018.10.074>.
- Hubbard, D.T. and Mavroeidis, G.P. (2011), "Damping coefficients for near-fault ground motion response spectra", *Soil Dyn. Earthq. Eng.*, **31**(3), 401-417. <https://doi.org/10.1016/j.soildyn.2010.09.009>.
- Hao, A., Zhou, D., Li, Y. and Zhang, H. (2011), "Effects of moment magnitude, site conditions and closest distance on damping modification factors", *Soil Dyn. Earthq. Eng.*, **31**(9), 1232-1247. <https://doi.org/10.1016/j.soildyn.2011.05.002>.
- Hatzigeorgiou, G.D. (2010), "Damping modification factors for SDOF systems subjected to near-fault, far-fault and artificial earthquakes", *Earthq. Eng. Struct. Dyn.*, **39**(11), 1239-1258. <https://doi.org/10.1002/eqe.991>.
- Kawashima, K. and Aizawa, K. (1986), "Modification of earthquake response spectra with respect to damping ratio", *Proceedings of the 3rd US National Conference on Earthquake Engineering*, Charleston, South Carolina, August.
- Khoshnoudian, F., Ahmadi, E. and Azad, A.I. (2014), "Damping coefficients for soil-structure systems and evaluation of FEMA 440 subjected to pulse-like near-fault earthquakes", *Soil Dyn. Earthq. Eng.*, **61-62**, 124-134. <https://doi.org/10.1016/j.soildyn.2014.02.009>.
- Kanno T., Narita A., Morikawa N., Fujiwara, H. and Fukushima, Y. (2006), "A new attenuation relation for strong ground motion in Japan based on recorded data", *Bull. Seism. Soc. Am.*, **96**(3), 879-897. <https://doi.org/10.1785/0120050138>.
- Lin, Y.Y. and Chang, K.C. (2003), "Study on damping reduction factor for buildings under earthquake ground motions", *ASCE J. Struct. Eng.*, **129**(2), 206-214. [https://doi.org/10.1061/\(ASCE\)0733-9445\(2003\)129:2\(206\)](https://doi.org/10.1061/(ASCE)0733-9445(2003)129:2(206)).
- Lin, Y.Y. and Chang, K.C. (2004), "Effects of site classes on damping reduction factors", *J. Struct. Eng.*, **130**(11), 1667-1675. [https://doi.org/10.1061/\(ASCE\)0733-9445\(2004\)130:11\(1667\)](https://doi.org/10.1061/(ASCE)0733-9445(2004)130:11(1667)).
- Lin, Y.Y., Miranda, E. and Chang, K.C. (2005), "Evaluation of damping reduction factors for estimating elastic response of structures with high damping", *Earthq. Eng. Struct. Dyn.*, **34**(11), 1427-1443. <https://doi.org/10.1002/eqe.499>.
- Lin, Y.Y. (2007), "Statistical study on damping modification factors adopted in Taiwan's seismic isolation design code by using the 21 September 1999 Chi-Chi earthquake, Taiwan", *Eng. Struct.*, **29**(5), 682-693. <https://doi.org/10.1016/j.engstruct.2006.06.006>.
- Li, H. and Chen, F. (2017), "Damping modification factors for acceleration response spectra", *Geod. Geodyn.*, **8**(5), 361-370. <https://doi.org/10.1016/j.geog.2017.04.009>.
- Mollaioli, F., Liberatore, L. and Lucchini, A. (2014), "Displacement damping modification factors for pulse-like and ordinary records", *Eng. Struct.*, **78**, 17-27. <https://doi.org/10.1016/j.engstruct.2014.07.046>.
- Nigam, N. and Jennings P. (1969), "Calculation of response spectra from strong-motion earthquake records", *Bull. Seism. Soc. Am.*, **59**(2), 909-922. <https://doi.org/10.1785/BSSA0590020909>.
- NEHRP (2000), Recommended Provisions for Seismic Regulations for New Buildings and Other Structures, Federal Emergency Management Agency, Washington D.C., USA.
- Newmark, N.M. and Hall, W.J. (1982), *Earthquake Spectra and Design EERI Monograph Series*, Earthquake Engineering Research Institute, Oakland, CA, USA.
- National Research Institute for Earth Science and Disaster Resilience (NIED) (1995), Strong Motion Seismograph Networks (K-NET, KIK-net). Accessed December 2020.
- Nagao, K. and Kanda, J. (2015), "Estimation of damping correction factors using duration defined by standard deviation of phase difference", *Earthq. Spectra*, **31**(2), 761-783. <https://doi.org/10.1193/103012EQS321M>.
- Papagiannopoulos, G.A., Hatzigeorgiou, G.D. and Beskos, D.E. (2013), "Recovery of spectral absolute acceleration and spectral relative velocity from their pseudo-spectral counterparts", *Earthq. Struct.*, **4**(5), 489-508. <http://dx.doi.org/10.12989/eas.2013.4.5.489>.
- Palermo, M., Silvestri, S. and Trombetti, T. (2016), "Stochastic-based damping reduction factors", *Soil Dyn. Earthq. Eng.*, **80**, 168-176. <https://doi.org/10.1016/j.soildyn.2015.09.014>.
- Pu, W., Kasai, K., Karoki, E.K. and Huang, B. (2016), "Evaluation of the damping modification factor for structures subjected to near-fault ground motions", *Bull. Earthq. Eng.*, **14**, 1519-1544. <https://doi.org/10.1007/s10518-016-9885-8>.
- Piscal, A.C.M. and López-Almansa, F. (2018), "Generating damping modification factors after artificial inputs in scenarios of local records scarcity", *Bull. Earthq. Eng.*, **16**, 1-26. <https://doi.org/10.1007/s10518-018-0406-9>.
- Rezaeian, S., Bozorgnia, Y., Idriss, I.M., Abrahamson, N., Campbell, K. and Silva, W. (2014), "Damping scaling factors for elastic response spectra for shallow crustal earthquakes in active tectonic regions: "Average" horizontal component", *Earthq. Spectra*, **30**(2), 939-963. <https://doi.org/10.1193/100512EQS298M>.
- Sadek, F., Mohraz, B. and Riley, M.A. (2000), "Linear procedures for structures with velocity-dependent dampers", *J. Struct. Eng.*, **126**(8), 887-895. [https://doi.org/10.1061/\(ASCE\)0733-9445\(2000\)126:8\(887\)](https://doi.org/10.1061/(ASCE)0733-9445(2000)126:8(887)).
- Sheikh, M.N., Tsang, H.H., Yaghmaei-Sabegh, S. and Anbazhagan, P. (2013), "Evaluation of damping modification factors for seismic response spectra", *Australian Earthquake Engineering Society Conference 2013*, Hobart, Tasmania, Australia, November.
- Surana, M., Singh, Y. and Lang, D.H. (2019), "Damping modification factors observed from the Indian strong-motion database", *J. Earthq. Eng.*, **25**(13), 2758-2773. <https://doi.org/10.1080/13632469.2019.1643809>.
- Stafford, P.J., Mendis, R. and Bommer, J.J. (2008), "Dependence of damping correction factors for response spectra on duration and numbers of cycles", *J. Struct. Eng.*, **134**(8), 1364-1373. [https://doi.org/10.1061/\(ASCE\)0733-9445\(2008\)134:8\(1364\)](https://doi.org/10.1061/(ASCE)0733-9445(2008)134:8(1364)).
- Tolis, S.V. and Faccioli, E. (1999), "Displacement design spectra", *J. Earthq. Eng.*, **3**(1), 107-125. <https://doi.org/10.1080/13632469909350342>.
- Wu, J.P. and Hanson, R.D. (1989), "Study of inelastic response spectra with high-damping", *J. Struct. Eng.*, **115**(6), 1412-1431. [https://doi.org/10.1061/\(ASCE\)0733-9445\(1989\)115:6\(1412\)](https://doi.org/10.1061/(ASCE)0733-9445(1989)115:6(1412)).
- Zhao, Y.G. and Zhang, H. (2017), "A simple approach for the fundamental period of MDOF structures", *Earthq. Struct.*, **13**(3), 231-239. <https://doi.org/10.12989/eas.2017.13.3.231>.
- Zhao, J.X., Yang, Q., Su, K., Liang, J., Zhou, J., Zhang, H. and Yang, X. (2019), "Effects of earthquake source, path, and site conditions on damping modification factor for the response spectrum of the horizontal component from subduction earthquakes", *Bull. Seism. Soc. Am.*, **109**(6), 2594-2613. <https://doi.org/10.1785/0120190105>.
- Zhou, J., Tang, K., Wang, H. and Fang, X. (2014), "Influence of ground motion duration on damping reduction factor", *J. Earthq. Eng.*, **18**(5), 816-830. <https://doi.org/10.1080/13632469.2014.908152>.
- Zhou, J. and Zhao, J.X. (2020), "A damping modification factor prediction model for horizontal displacement spectrum from

- subduction interface earthquakes in Japan accounting for site conditions”, *Bull. Seism. Soc. Am.*, **110**(3), 1231-1246. <https://doi.org/10.1785/0120190275>.
- Zhang, H. and Zhao, Y.G. (2020), “Damping modification factor based on random vibration theory using a source-based ground-motion model”, *Soil. Dyn. Earthq. Eng.*, **136**, 106225. <https://doi.org/10.1016/j.soildyn.2020.106225>.
- Zhang, H. and Zhao, Y.G. (2022a), “Damping modification factor of acceleration response spectrum considering seismological effects”, *J. Earthq. Eng.*, **26**(16), 8359-8382. <https://doi.org/10.1080/13632469.2021.1991521>.
- Zhang, H. and Zhao, Y.G. (2022b), “An analytical model for displacement response spectrum considering the soil-resonance effect”, *Earthq. Struct.*, **22**(4), 373-386. <https://doi.org/10.12989/eas.2022.22.4.373>.

Appendix A

DMF	Damping modification factor
$DMF(T_{\min})$	Minimum value of DMF
T_0	Oscillator period
$V_{S,30}$	Shear-wave velocity in the upper 30m
h_i	Thickness of the i th layer of soil
M	Magnitude
PSa	Pseudo-acceleration response spectrum
$PSa(5\%, T_0)$	Pseudo-acceleration response spectrum at a damping ratio of 5%
$Sd(5\%, T_0)$	Displacement response spectrum at a damping ratio of 5%
T_c^*	Spectral shape factor expressed by Eq. (5)
Ω	Spectral shape factor expressed by Eq. (7)
S_v	Velocity response spectrum
λ_1^*	First moment of S_v expressed by Eq. (9)
k_0	Parameter controlling the increasing rate of DMF with the period at $T_0 > T_{\min}$
a and b	Regression coefficients of Eq. (15)
PGA	Peak ground acceleration
T_{\min}	Oscillator period corresponding to $DMF(T_{\min})$
ζ	Oscillator damping ratio
$V_{S,20}$	Shear-wave velocity in the upper 20m
V_i	Shear-wave velocity of the i th layer of soil
R	Distance
$PSa(6s)$	Value of the pseudo-acceleration response spectrum at 6s
$PSa(\zeta, T_0)$	Pseudo-acceleration response spectrum at a damping ratio of ζ
$Sd(\zeta, T_0)$	Displacement response spectrum at a damping ratio of ζ
T_{cen}^*	Spectral shape factor expressed by Eq. (6)
p	Spectral shape factor expressed by Eq. (11)
λ_0^*	Zeroth moment of S_v expressed by Eq. (8)
λ_2^*	Second moment of S_v expressed by Eq. (10)
c	Regression coefficients of Eq. (12)
T_R and α	Regression coefficients of Eq. (17)